Comparison Between Calculated and Measured Cross Section Changes in Natural Uranium Irradiated in NRX

P-E. Ahlström

AE-43

AKTIEBOLAGET ATOMENERGI

STOCKHOLM · SWEDEN · 1961

COMPARISON BETWEEN CALCULATED AND MEASURED CROSS-SECTION CHANGES IN NATURAL URANIUM IRRADIATED IN NRX

P-E Ahlström

Summary

It is desirable to obtain an experimental check of the reliability of the methods currently used to determine reactivity changes in a reactor and, with a view to meeting this requirement to some extent, a preliminary comparison has been made between calculated and measured cross-section changes in rods of natural uranium irradiated in NRX. The measurements were made at Harwell in the GLEEP reactor and a description has been given by, inter alia, Ward and Craig. The theory of the calculations, which is briefly described in this report, has been indicated by Littler.

The investigation showed that the methods for calculating burn up used at present provides a good illustration of the long-term variations in isotope contents. A satisfactory agreement is obtained with experimental results when calculating apparent cross-section changes in uranium rods due to irradiation if the fission cross-section for Pu^{239} is set to 780b. This is 34 b higher than the figure quoted in BNL - 325 (1958). However, in order to get a good idea as to whether the calculated long-term variations in reactivity really correspond to reality, it is necessary to make further investigations. For this reason the results quoted in this report should be regarded as preliminary.

Printed March 1961

Comparison between calculated and measured cross-section changes in natural uranium irradiated in NRX.

List of contents

1. Introduction

It is desirable to obtain an experimental check of the reliability of the methods currently used when calculating reactivity changes in a reactor (2 and 3) and, with a view to meeting this requirement to some extent, a comparison has been made between calculated and measured cross-section changes in samples of natural uranium metal irradiated in NRX. The measurements used when making the comparison are described by Ward and Craig (1.)

2. Theory of calculations

Measurement of the cross-section changes has been carried out by

1) measuring the effective cross-section of the sample in the GLEEP reactor at Harwell
2) irradiating the sample in NRX
3) measuring the effective cross-section of the irradiated sample in GLEEP
4) calculating the difference between the results of 1) and 3).

This difference is a direct measurement of the reactivity change in GLEEP.

When calculating the measured quantity it is necessary to determine the change in the composition of the sample. This depends on the neutron flux and neutron spectrum during irradiation and on the cross-sections of the existing isotopes. The calculation of the change in the composition of the sample has been made with the aid of the burn up code (2 and 3). This gives the macroscopic cross-sections of isotopes U^{235}, U^{236}, U^{238}, Pu^{239}, Pu^{240}, Pu^{241} and the fission products. These cross-sections must then be converted to cross-section change in GLEEP in accordance with the following formula.

$$\sum_{app} \cdot \frac{\phi_o}{\phi} = \frac{1 + \Delta \phi/\phi}{N^o_{25} + N^o_{49} + N^o_{41}} \sum_{ik} N_{ik} \hat{\sigma}_{ik} (1 - w^1 \epsilon \eta_{ik})$$

$$\frac{1}{N^o_{25} + N^o_{49} + N^o_{41}} \sum_{ik} N^o_{ik} \hat{\sigma}^o_{ik} (1 - w^1 \epsilon \eta_{ik}^o)$$

$\sum$ app = measured or calculated cross-section change in bifa (barns per initial fissile atom)

ϕ_o = mean neutron flux in sample position without sample
ϕ = " " " " " " with non-irradiated sample
$\phi + \Delta\phi$ = " " " " " " " irradiated sample
N^o_{ik} = content of isotope ik before irradiation
N_{ik} = " " " " after irradiation
$\hat{\sigma}^o_{ik}$ = effective cross-section of ik in GLEEP before irradiation
$\hat{\sigma}_{ik}$ = " " " " " " after irradiation
σ_{ik} = " mean cross-section of ik in NRX during irradiation
ϵ = fast fisson factor in GLEEP
w^1 = weight of a fast fission neutron compared with a thermal neutron in GLEEP

Summations are made in respect of all isotopes occurring in the fuel. The relative change in flux between non-irradiated and irradiated samples is calculated in the manner shown below (4).

$$-\frac{\Delta\phi}{\phi} \cdot \sum_{ik} N^o_{ik}\ \hat{\sigma}^o_{ik} = \alpha \sum_{ik} (N_{ik}\ \hat{\sigma}_{ik} - N^o_{ik}\ \hat{\sigma}^o_{ik}) +$$

$$+ \beta \sum_{ik} (N_{ik}\ \hat{\sigma}_{ik}\ \eta_{ik} - N^o_{ik}\ \hat{\sigma}_{ik}\ \eta^o_{ik}) + \gamma\ (N_{49}\ \hat{\sigma}_{49} - N^o_{49}\ \hat{\sigma}^o_{49}) +$$

$$+ \delta\ (N_{40}\ \hat{\sigma}_{40} - N^o_{40}\ \sigma^o_{40})$$

Constants $\alpha, \beta, \gamma, \delta$ are allocated the following values by Craig and others (4)

α = - 0, 66
β = 0, 13
γ = 0, 04
δ = 0, 22

These magnitudes are typical for GLEEP, see also (5). In addition

$$\eta_{ik} = \frac{\hat{\sigma}_{fik}}{\hat{\sigma}_{ik}} \cdot \nu_{ik}$$

and

$$\eta^{o}_{ik} = \frac{\hat{\sigma}^{o}_{fik}}{\hat{\sigma}^{o}_{ik}} \quad \nu_{ik}$$

where

$\hat{\sigma}^{o}_{fik}$ = the effective fission cross-section of ik in GLEEP before irradiation

$\hat{\sigma}_{fik}$ = ditto after irradiation

ν_{ik} = average number of neutrons formed on fission of one nucleus of ik.

The isotope contents N^{o}_{ik} and N_{ik} are calculated from $\sigma_{ik} \cdot N_{ik}$ and σ_{ik}, which are obtained from the burn up code (2 and 3), except for Sm^{149}. When the first calculations were made it was assumed that this isotope had a macroscopic cross-section constant in time. However, it was found that this condition can hardly be satisfied since the agreement with the experimentally determined values of $\sum_{app}$ was very poor. N_s was then calculated as follows.

$$N_s = \frac{P_o + S_o}{b} (1 - e^{-bt}) + \frac{P_o}{b - a} (e^{-bt} - e^{-at})$$

$$+ \frac{P_o}{\lambda_p} (1 - e^{-at}) (1 - e^{-\lambda_p' t})$$

$$P_o = \frac{\lambda_p \cdot F}{\sigma_p \cdot F + \lambda_p} \sum_{ik} \gamma_{pik} \cdot \sigma_{fik} \cdot N_{ik}$$

$$S_o = F \sum_{ik} \gamma_{sik} \cdot \sigma_{fik} \cdot N_{ik}$$

$$a = \lambda_p + \sigma_p \cdot F$$

$$b = \sigma_s \cdot F$$

$$\tau = t \cdot F$$

The indices denote

$p = Pm^{149}$

$s = Sm^{149}$

f = fission cross-section

In addition

λ_j	=	decay constant of isotope j
γ_{jik}	=	yield of isotope j from fission of one isotope ik
F	=	mean flux in sample being irradiated
t	=	irradiation time
τ	=	irradiation
t'	=	time between completed irradiation and measurement of cross-section after irradiation.

The above formulae were programmed for calculation on the FACIT EDB machine by A. Lock, Swedish State Power Board. The programme can handle 7 different isotopes plus one term for all fission products except Sm^{149}, which is dealt with as above. Details of the programme are shown in App. 1.

A comprehensive description of the theory of these measurements is given by Littler (5).

3. Calculations

The calculations with the burn up programme have been made with the assumptions described in ref. 3. Table 1 shows the data for NRX and for the irradiated samples. The resonance escape probability of U^{238} (P_{28}) has been calculated by means of formula

$$P_{28} = 1 \frac{ICR - \sigma_{28}N^o_{28}/\sigma_{25}N^o_{25}}{\eta_{25} \cdot \epsilon \cdot e^{-B_g^2 \tau_f}} +$$

$$+ \frac{\alpha_{28}(\epsilon - 1)}{\nu_{28} - 1 - \alpha_{28}} \cdot \frac{1}{\epsilon \cdot e^{-B_g^2 \tau_f}}$$

where ICR = 0.76 according to Craig and others (4) and the other data are shown in Table 1 or ref. 3. The effective surface of the sample rods for the resonance absorption in Pu^{240} has been taken as being the same as the total surface. When making the calculations the values for the effective cross-sections in GLEEP of the various isotopes have been assumed to be same as those indicated by Craig and others (4). These values are shown in Table 2.

The correction factor ϕ_o/ϕ has been introduced by Craig and Ward (1) into the experimental Σ_{app}-values and thus this factor has been taken as = 1 in the calculations.

The yields of Sm^{149} upon fission of various nuclei has been assumed to be zero, while yields of Pm^{149} has been set at

$$\gamma_{p25} = 0.0115$$

$$\gamma_{p49} = 0.018$$

$$\gamma_{p41} = 0.019$$

The decay constant for Pm^{149} is

$$\lambda_p = 0.370 \cdot 10^{-5} \ s^{-1}$$

and the effective cross-section of the same isotope is negligible for practical purposes. The effective cross-section of Sm^{149} in GLEEP is stated by Craig and others (4) to be 72700 b. The corresponding cross-section during irradiation has been calculated from Westscott's tables (8). Assuming the effective neutron temperature to be 61°C, the effective r-factor 0.07 and $\sigma_s^{2200} = 40,800$ barns (according to BNL-325 1958) we get $\sigma_s = 67,980$ b, which has been used in the calculations.

The time t has been set to 1 year, which means that all prometium stored in the fuel when irradiation ceased is assumed to have decayed to samarium. When making the comparative calculations the neutron flux was set at 10^{13} n/cm^2 s, but when making a final calculation on each of the irradiated samples the values given by Ward

and Craig (1) were used.

The quantity Σ_{app} has been calculated for different irradiations and the results have been compared with the experimental values given by Ward and Craig (1). The latter values are corrected for the decay of Pm^{149}, Eu^{155}, Np^{239} and Pu^{241} during the time between irradiation and the second measurement in GLEEP. When making the comparison the correction for Pm^{149} decay has not been included since the model used for the calculation of the Sm^{149} action makes allowance for it. In order to obtain agreement between the measured and the calculated values the fission cross-section for Pu^{239} has been varied. All the other cross-sections have been kept constant, this being especially the case with the capture cross-section for Pu^{239}. This means that the absorption cross-section has been altered by the same absolute amount as the fission cross-section. Corresponding changes in the cross-sections have also been made in Table 2. The results of these calculations are shown on graphs 1 and 2.

In order to be able to study the influence of the uncertainty of the r-factor (relative strength of epithermal spectrum) this factor has been varied while keeping all the other quantities constant. The results are shown by the dotted curves and curve 4 in graph 1. A quick inspection of graph 1 shows that curve 5 or 6 provide the best agreement with the experimental points. However, the measurements have been carried out on samples which have been irradiated with very different neutron fluxes. This has a great effect on the accumulated amount of Pm^{149} which after irradiation has ceased decays to Sm^{149}. For this reason the change in cross-section has been calculated for each of the 42 samples included in Ward and Craig's list (1). It is found that the experimental values and the theoretical values agree fairly well if we allow that $\sigma^{2200} = 780$ barns and that $r = 0.07$ as per case 4 on graphs 1 and 2.^{49f} A summary of the results of the calculations in this case is given in tables 3 and 4. The first table refers to 18 samples (Series I in ref. 1) and the second to 24 samples (Series II and III in ref. 1). The sample numbers, irradiation (τ) and the neutron flux (ϕ) have been taken direct from Tables 1 and 2 in ref. 1. Σ_{app} are the values given in the next but last column in these tables corrected for the decomposition of Np-239, Eu-155 and Pu-241. In Tables 3 and 4 various types of mean deviations have been calculated from the differences shown in the table between the calculated and measured cross-section changes.

It will be seen from Table 4 that sample 13 shows an unexpectedly large difference from the others, this indicating that an accidental error has crept in when making the measurement. Disregarding this sample the deviations are those shown in brackets. A calculation of the mean deviations for all 42 (41) samples gave the following results.

$$\frac{1}{n}\sum_{\nu=1}^{n}\Delta\Sigma_{\nu} = -\ 0.15\ (-\ 0.03) \qquad \text{bifa}$$

$$\frac{1}{n}\sum_{\nu=1}^{n}\left|\Delta\Sigma_{\nu}\right| = 0.71\ (0.60) \qquad "$$

$$\sqrt{\frac{1}{n}\sum_{\nu=1}^{n}\left|\Delta\Sigma_{\nu}^{2}\right|} = 1.16\ (0.83) \qquad "$$

The measurement accuracy in Σ_{app}^{exp} is quoted by Ward and Craig (1) as being $\pm$ 0.13 bifa.

The isotope composition of 5 of the irradiated samples has been determined experimentally by Hart and others (9). The results of their work, and the calculated curves, have been drawn on graphs 3 and 4. The accuracy of the experimental determinations is relatively good. Using the error limits given in ref. 9 the quadratic mean errors of the measuring points on graph 3 have been calculated as being about 1% for Pu^{239} and about 2% for Pu^{241}. The uncertainty factor in the irradiation has not been included. According to Ward and Craig (1) this is about 2%, but an additional correction must be made for changed flux depression over the sample rods during irradiation. This correction is stated as being about - 0.02 n/kb at irradiation 0.6 n/kb.

The calculated long-term variation in the isotope contents is little influenced by the assumption in respect of the fission cross-section for Pu^{239}. This is clearly shown in graph 3, in which two curves with 746 and 800 barns for σ_{49f}^{2200} have been inserted for every quantity. In the case of the calculation model used the change in U^{235} content with irradiation is unaffected by this assumption.

No details have been published of the variation in Sm^{149} con-

centration when irradiating the fuel.

4. Discussions and conclusions

It must be emphasized that this comparison between the theoretical and the experimental changes in cross-section merely confirm that the calculations of the long-term variations in isotope contents are pretty well correct. On the other hand, it gives no indication as to how the estimated changes of reactivity in the reactor where the samples were irradiated derived from these variations agree with actual conditions. True, the quantity Σ_{app} is a measurement of reactivity change in GLEEP, but the latter is graphite-moderated and of low power and, furthermore, differs in several other ways from NRX. Consequently separate cross-sections for the isotopes in GLEEP must be calculated. In this comparison the calculated cross-section values for GLEEP presented by Craig and others (4) have been used. These are determined in accordance with a more complicated calculation model than that used in the burn up code (2, 3). In order to be able to check the determination of the change in reactivity by this method it should also be used to calculate the cross-sections in GLEEP. The intention is to do this at a later date.

In order to be able to suit the calculated Σ_{app} to the measured values it was decided to vary the fission cross-section of Pu^{239}. This choice may seem to be purely arbitrary and it is, of course, possible to obtain a good adjustment by choosing another parameter. However, the essential change in reactivity when irradiating uranium is due to the formation of Pu^{239} and fission products. However, the cross-sections of the latter are hardly suitable as parameters and the simplest way would seem to be to choose one of the Pu^{239} cross-sections. Changes in the latter should then be effected in such a way as to obtain a change in the η-value at the same time. This provides great sensitivity to small changes. In the case of higher irradiations than those investigated the contents of Pu^{240} and Pu^{241} become appreciable and in that case it may be possible to use the cross-section of one of these isotopes as the parameter.

As will be seen from graph 3 the isotope contents are very immune to variations in σ_{49f}^{2200}. On the other hand, as has already been mentioned and as is shown by graph 2, Σ_{app} is sensitive to even small changes in σ_{49f}^{2200}. This is due to the fact that the η -value of Pu^{239} is changed and that the calculated Σ_{app} is, absolutely, a small difference between several large figures, each of which represents the change in cross-section of one of the component isotopes.

The investigation showed that the long-term variation in the Sm^{149} content has a marked influence on the reactivity changes. When starting a reactor with fresh fuel (natural U) the Sm^{149} concentration increases rapidly from zero to a quasi-stationary value. As the Pu content grows this value increases also. The reason is that yield of Sm^{149} is greater from the fission of Pu^{239} and Pu^{241} than from the fission of U^{235}. When the reactor is started and stopped the extent of the neutron flux will influence the size of the reactivity transients obtained. In this connection it should be pointed out that the calculation model used in this particular case for determining the influence of Sm^{149} assumes that, on starting, the transients are rapid in relation to the changes in Pu contents. Whether or not this assumption is satisfactorily covered has not been fully investigated, but graph 3 would appear to indicate that this is not the case. For this reason this effect and other effects in other fission products and also Np^{239} will be investigated more closely in connection with the development of a new reactivity change code.

The calculated change in reactivity depends very greatly upon the assumed η-value for Pu^{239} (η_{49}). This is illustrated by graph 5, in which the calculated value of Bm_2 (for NRX) is expressed as a function of the reactivity change with η_{49} (eg. σ_{49f}^{2200}) as the parameter. As will be seen differences of about 500 MWd/tU are obtained at changes of 1% in η_{49}^{2200}.

In conclusion it can be said that the burn up code used here gives a good illustration of the long-term variations in the isotope contents. A satisfactory agreement is also obtained with experimental results when calculating the apparent changes in cross-section of irradiated uranium rods if the fission cross-section of Pu^{239} is set to 780 b, and the other used are as indicated in ref. 3. However, in order to get a good idea as to the extent to which the calculated

long-term variations in reactivity agree with actual conditions it will be necessary to carry out further investigations. For this reason the results shown in this report should be regarded as preliminary.

5. References

1. WARD A G, CRAIG D S
Measurements of the reactivity change with irradiation for natural uranium samples irradiated in NRX
AECL-812 (CRRP-761-A), (1959)

2. AHLSTRÖM P-E
Utbränningsberäkningar för en termisk reaktor
AB Atomenergi RFR-10 (1958)

3. AHLSTRÖM P-E
Ändringar i programmet för utbränningsberäkningar
Statens Vattenfallsverk PM A-43/59 (1959)

4. CRAIG D S, HANNA G C, HURST D G, KUSHNERIUK S A, LEWIS W B, WARD A G
Long Irradiation of Natural Uranium
A/CONF. 15/P/205 (1958)

5. LITTLER D J
Measurements of the Change in Cross Section of Irradiated Uranium made by Moderating the Power of a Nuclear Reactor
A.E.R.E. RS/S 2092 (1956)

6. Reactors of the world: NRX, Särtryck ur Nuclear Engineering

7. KUSHNERIUK S A
Effective Cross-Sections and Neutron Flux Distributions in a Natural Uranium Rod. Application to rod 683.
AECL-497 (CRT-725) (1957)

8. WESTCOTT C H, ROY C A
Supplement to "Effective Cross Section Values for Well-Moderated Thermal Reactor-Spectra"
CRRP-862 (1958)

9. HART R G, LOUNSBURY M, BIGHAM C B, CORRIVEAU L P V, GIRARDI F
Chemical and Isotopic Analysis of Irradiated Uranium Slugs from Demountable Slug Rod A.G.W.-1
(P-4498), A.E.C.L.-813 (CRRP-761-B) (1959)

Table 1

Data for NRX and for irradiated samples used in the burn up programme.

Quantity	Value used	Unit	Reference
Length of sample	15.24	cm	1
Diameter of sample	3.455	"	1
f	0.928		6
ϵ	1.036		6
η	1.318		calculated
p_{28}	0.91		"
L^2	156	cm^2	6
τ_f	114	"	6
B_g^2	$4.07 \cdot 10^{-4}$	cm^{-2}	6
ICR (best value)	0.760 ± 0.008		4
Moderator temperature	38	^oC	
$\sqrt{\frac{S_{eff}}{M}}$	0.265	$cm/\sqrt{g}$	calculated
Density of sample	18.97	g/cm^3	
Moderator volume/fuel volume	24.6		7 (p. 18-19)

Table 2

Effective cross-sections in GLEEP

Irradiation n/kb	Pu^{239}		Pu^{240}
	$\hat{\sigma}_{49}$ b	$\hat{\sigma}_{49f}$ b	$\hat{\sigma}_{40}$ b
0	1383	929	1473
0.1	1364.9	918.2	1393
0.2	1349.5	909.6	1251
0.3	1336.3	902.6	1105
0.4	1327.7	897.2	984
0.5	1319.5	892.4	889
0.6	1312.7	888.7	816
0.7	1307	885.7	711

	$\hat{\sigma}_{ik}$ b	$\hat{\sigma}_{ikf}$ b	
U^{235}	666.9	555.6	assumed to be independent of irradiation
Pu^{241}	1500	1100	

Table 3

Sample No.	τ n/kb	ϕ n/cm^2 s	Σ_{app}^{exp} bifa	Σ_{app}^{ber} bifa	$\Delta\Sigma_{app}$	$(\Delta\Sigma_{app})^2$
2	0.00160	0.113	0.78	0.599	- 0.181	0.03276
3	0.00355	0.251	1.65	1.249	- 0.401	0.16080
4	0.0078	0.551	2.86	2.475	- 0.385	0.14823
5	0.0119	0.84	3.98	3.331	- 0.649	0.42120
6	0.0148	1.05	4.20	3.889	- 0.311	0.09672
7	0.0178	1.26	4.55	4.362	- 0.188	0.03534
8	0.0210	1.49	4.42	4.788	+ 0.368	0.13542
9	0.0220	1.56	4.76	4.901	+ 0.141	0.01988
10	0.0241	1.71	5.37	5.138	- 0.232	0.05382
11	0.0239	1.69	4.72	5.113	+ 0.393	0.15445
12	0.0241	1.71	4.76	5.138	+ 0.378	0.14288
13	0.0247	1.75	5.24	5.191	- 0.049	0.00240
14	0.0216	1.53	4.89	4.853	- 0.037	0.00137
15	0.0199	1.41	4.42	4.653	+ 0.233	0.05429
16	0.0171	1.21	4.33	4.621	+ 0.291	0.08468
17	0.0136	0.96	3.68	3.685	+ 0.005	0.00003
18	0.0098	0.69	3.46	2.922	- 0.538	0.28944
19	0.0056	0.40	2.25	1.859	- 0.391	0.15288

$$\frac{1}{18}\sum_{2}^{19} \Delta\Sigma = -\frac{1.553}{18} = -\underline{0.0863}$$

$$\frac{1}{18}\sum_{2}^{19} |\Delta\Sigma| = -\frac{5.171}{18} = -\underline{0.287}$$

$$\sqrt{\frac{1}{18}\sum_{2}^{19} (\Delta\Sigma)^2} = \sqrt{\frac{1.986605}{18}} = \sqrt{0.110367} = \underline{0.332}$$

Table 4

Sample No.	$\bar{\tau}$ n/kb	$\bar{\phi}$ n/cm^2 s	Σ_{app}^{exp} bifa	Σ_{app}^{ber} bifa	$\Delta\Sigma_{app}$	$(\Delta\Sigma_{app})^2$
7	0.0160	0.52	3.67	3.625	- 0.045	0.002025
16	0.0225	0.73	3.73	4.165	+ 0.435	0.189225
31	0.0321	0.36	3.59	3.697	+ 0.107	0.011449
8	0.0347	1.12	3.92	4.534	+ 0.614	0.376996
24	0.0428	0.47	2.79	3.199	+ 0.409	0.167281
19	0.0529	0.51	1.73	2.809	+ 1.079	1.164241
12	0.0810	2.62	4.62	4.096	- 0.524	0.274576
5	0.0924	2.99	5.12	4.024	- 1.096	1.201216
32	0.0932	1.03	0.80	1.167	+ 0.367	0.134689
20	0.1158	1.12	0.14	0.618	+ 0.478	0.228484
26	0.1416	1.57	- 0.96	0.891	+ 1.851	3.426201
17	0.1523	0.68	- 0.94	- 0.662	+ 0.278	0.077284
9	0.2268	1.69	- 0.28	- 0.137	+ 0.143	0.020449
34	0.2660	2.95	0.36	2.338	+ 1.978	3.912484
29	0.2755	3.06	0.64	2.602	+ 1.962	3.849444
15	0.2879	1.28	1.32	- 0.047	- 1.367	1.868689
18	0.3173	2.36	3.93	2.575	- 1.355	1.836025
11	0.3840	2.86	6.86	5.864	- 0.996	0.992016
14	0.4059	1.81	5.65	5.203	- 0.447	0.199809
10	0.4793	2.14	10.16	9.910	- 0.250	0.062500
(13	0.5129	2.29	17.49	12.212	- 5.278	27.857284)
21	0.5167	2.67	12.94	13.143	+ 0.203	0.041209
3	0.5624	2.51	16.99	16.026	- 0.964	0.929296
4	0.6326	2.82	23.63	21.279	- 2.351	5.527201

$$\frac{1}{24}\sum_{7}^{4} \qquad \Delta\Sigma = -\frac{4.769}{24} = -\ 0.199 \quad (+\ 0.022)$$

$$\frac{1}{24}\sum_{7}^{4} \qquad \left|\Delta\Sigma\right| = \frac{24.577}{24} = 1.024 \quad (0.839)$$

$$\sqrt{\frac{1}{24}\sum_{7}^{4} (\Delta\Sigma)^2} = \sqrt{\frac{54.350073}{24}} = \sqrt{2.2646} = 1.505 \quad (1.073)$$

Operation of Programme 7665

Tape: Earliest date 9.10.1959.

Operation "0-MS", "Start from tape". Insert data tape, "Start". After recording stop with ASOP = 00130. At "Start" insertion of new data without datum and new calculation.

Data: Need only be punched up to and including the last change in each sequence. However, at least 1 datum is to be punched in each sequence. Telex punching (MNA's 904).

Recording If programme correctly inserted:

07220 07665
28008 01958
0*F

Results: Datum;

Recorded if $\neq 0$ in pos. 29:

Problem No.; τ; Σ_{app};

N_{25}; N_{26}; N_{28}; N_{49}; N_{40}; N_{41}; N_{42};

N^{o}_{25}; N^{o}_{26}; N^{o}_{28}; N^{o}_{49}; N^{o}_{40}; N^{o}_{41}; N^{o}_{42};

N_{sm}; $\frac{\Delta \phi}{\phi}$;

Instruction for punching of data for 7665

Punch	Pos.	Magnitude
230959	1.	Datum (only with first sequence)
11	2.	Problem No.
0.1016 E + 21	3.	τ
0.217275	4.	$\sigma_{25} \cdot N_{25} = X$
0.000095	5.	$\sigma_{26} \cdot N_{26} = Y$
0.022134	6.	$\sigma_{49} \cdot N_{49} = Z$
0.000082	7.	$\sigma_{40} \cdot N_{40} = U$
0.000016	8.	$\sigma_{41} \cdot N_{41} = V$
0.000950	9.	$\sigma_{FP} \cdot N_{FP} = W$
0	10.	$\sigma_{42} \cdot N_{42} = R$
0.13095	11.	$\sigma_{28} \cdot N_{28} = S$
672.69 E-24	12.	σ_{25}
25 E-24	13.	σ_{26}
2.748 E-24	14.	σ_{28}
1312,4 E-24	15.	σ_{49}
232 E-24	16.	σ_{40}
1589,5 E-24	17.	σ_{41}
1 E-24	18.	σ_{42}
0.232645	19.	X_o
0	20.	Y_o
0	21.	Z_o
0	22.	U_o
0	23.	V_o
0	24.	R_o
0.13095	25.	S_o
2.47	26.	ν_{25}
2.90	27.	ν_{49}
3.06	28.	ν_{41}
1 T	29.	End of number sequence
918 E-24	30.	$\hat{\sigma}_{f49}$
1100 E-24	31.	$\hat{\sigma}_{f41}$
1365 E-24	32.	$\hat{\sigma}_{49}$
1392 E-24	33.	$\hat{\sigma}_{40}$
1500 E-24	34.	$\hat{\sigma}_{41}$

Punch	Pos.	Magnitude
1 E-24	35.	$\hat{\sigma}_{42}$
555, 6 E-24	36.	$\hat{\sigma}_{f25}$
666, 9 E-24	37.	$\hat{\sigma}_{25}$
25 E-24	38.	$\hat{\sigma}_{26}$
2, 748 E-24	39.	$\hat{\sigma}_{28}$
555, 6 E-24	40.	$\hat{\sigma}^{o}_{f25}$
929 E-24	41.	$\hat{\sigma}^{o}_{f49}$
1100 E-24	42.	$\hat{\sigma}^{o}_{f41}$
666, 9 E-24	43.	$\hat{\sigma}^{o}_{25}$
25 E-24	44.	$\hat{\sigma}^{o}_{26}$
1383 E-24	45.	$\hat{\sigma}^{o}_{49}$
1473 E-24	46.	$\hat{\sigma}^{o}_{40}$
1500 E-24	47.	$\hat{\sigma}^{o}_{41}$
1 E-24	48.	$\hat{\sigma}^{o}_{42}$
2.748 E-24	49.	$\hat{\sigma}^{o}_{28}$
0.847	50.	W
1.036	51.	ϵ
- 0.66	52.	α
0.13	53.	β
0.04	54.	γ
0.22	55.	δ
1 E-24	56.	$\phi_o / \phi \cdot 10^{-24}$
T	57.	End of number sequence
0.0115	58.	γ_{p25}
0.018	59.	γ_{p49}
0.019	60.	γ_{p41}
560, 56 E-24	61.	σ_{f25}
898, 85 E-24	62.	σ_{f49}
1154, 74 E-24	63.	σ_{f41}
0	64.	γ_{S25}
0	65.	γ_{S49}
0	66.	γ_{S41}
1.0 E + 13	67.	F

Punch	Pos.	Magnitude
0.370 E-5	68.	λ_p
0	69.	σ_p
68100 E-24	70.	σ_{Sm}
72700 E-24	71.	$\hat{\sigma}_{Sm}$
8.64 • E + 6	72.	t'
T	73.	End of number sequence

$\Sigma_{app} = f(\tau)$ $0.1 \leq \tau < 0.7$

calculated and measured values

Graph 1

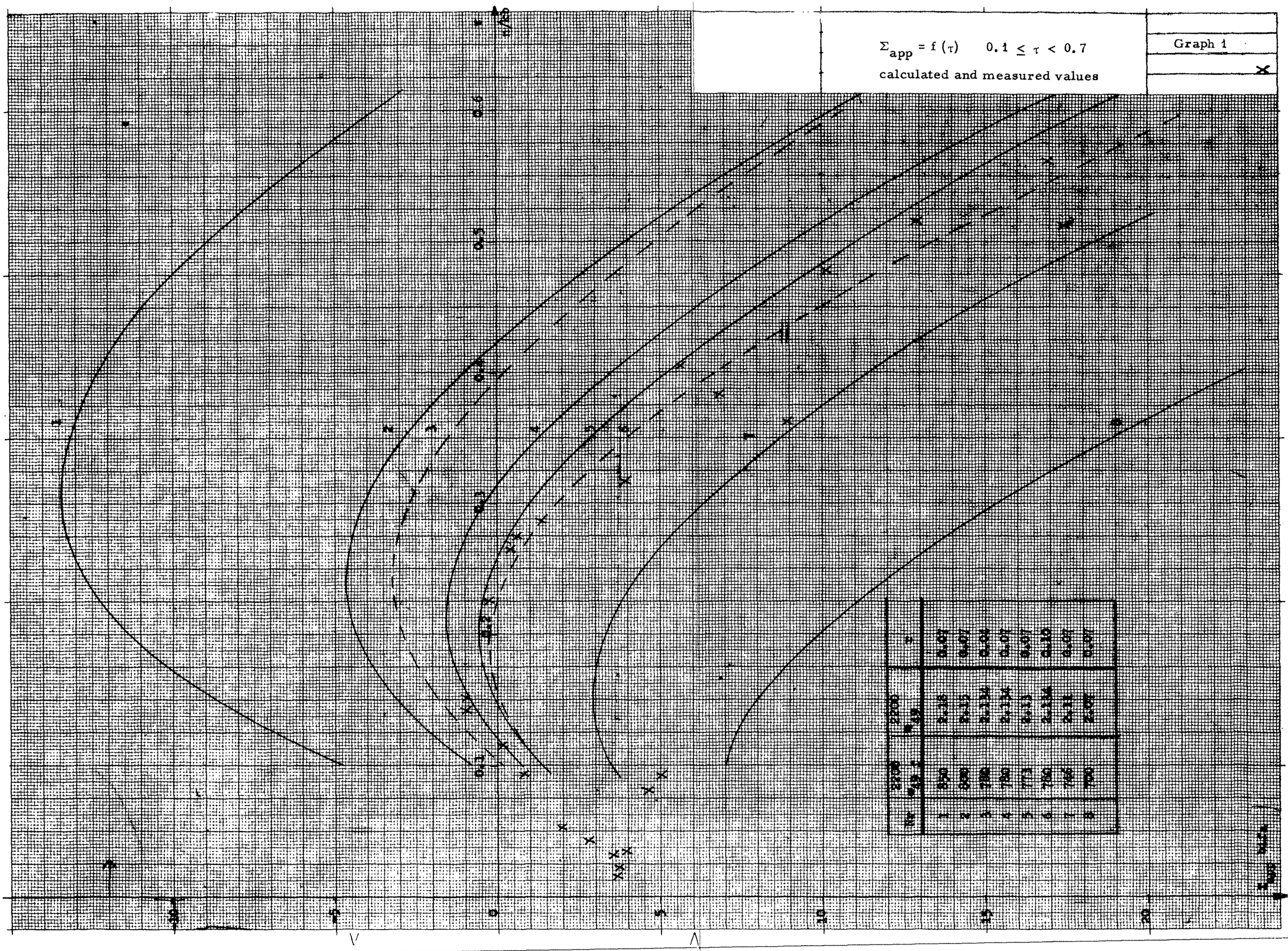

$\Sigma_{app} = f(\tau)$ $0 \leq \tau < 0.125$

calculated and measured values

Graph 2

0.325 cm/kb

0.300

0.275

0.250

0.225

V

Λ

N_{1k}/N_{25}°

0.35

0.30

0.25

0.20

0.15

0.10

0.05

0

2200 kg/cm² — 49 t

2200 kg/cm² — 49

746 kg/cm² — 2.11

800 kg/cm² — 2.15

□ $100 \cdot N_{41}/N_{25}^{\circ}$

△ $10 \cdot N_{40}/N_{25}^{\circ}$

○ N_{49}/N_{25}°

$1000 \cdot N_{3}/N_{25}^{\circ}$

0 0.1 0.2 0.3 0.4 0.5 0.6

t n/kb²

$N^{ik}/N_o^{25} = f(E)$ calculated and measured values

Graph 3

$N_{25}/N_{25}^{o} = f\ (\tau)$

calculated and measured values

Graph 4

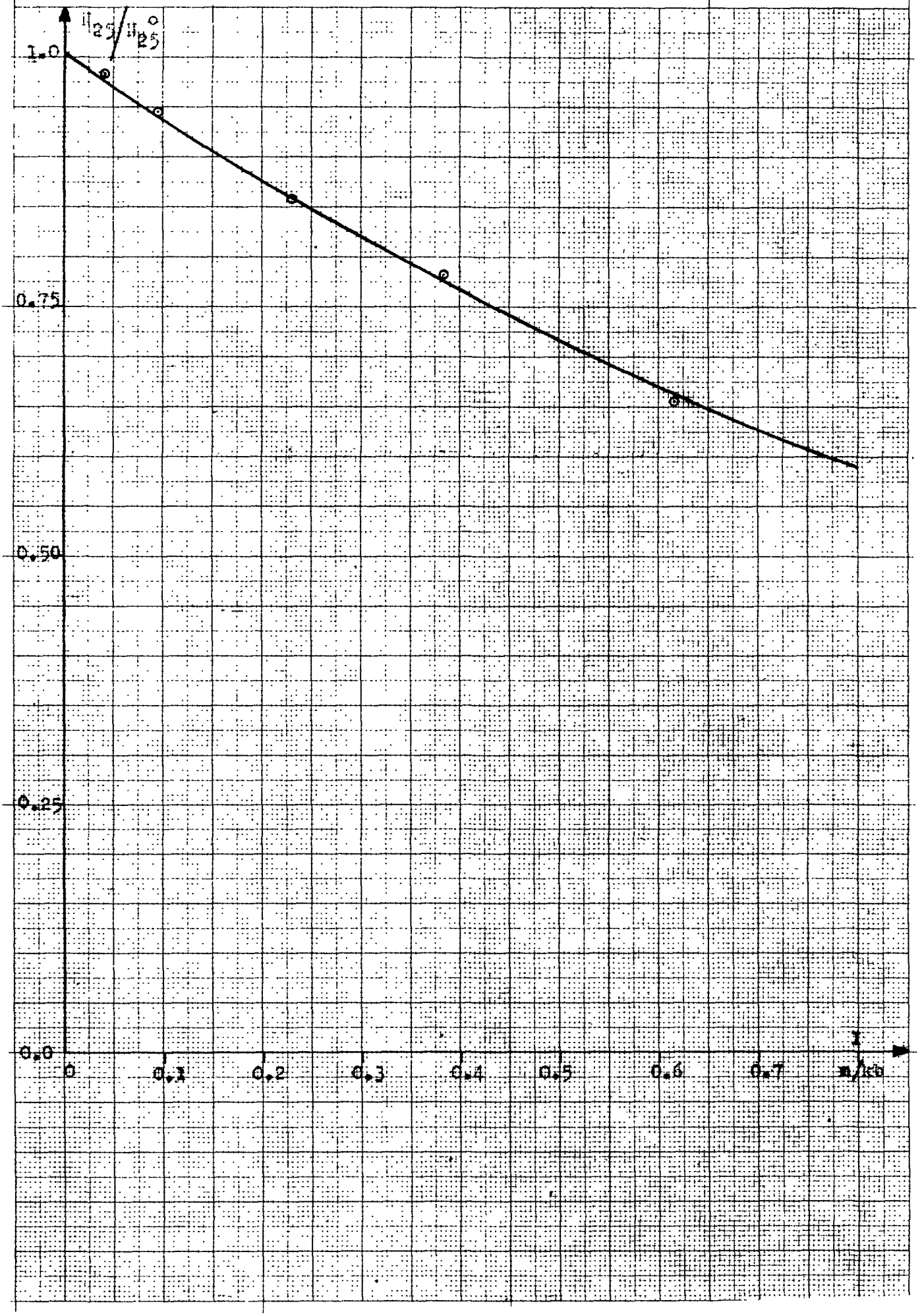

B_m^2 = f (E) for NRX calculated values,

non-correlated lattice calculation methods

Graph 5

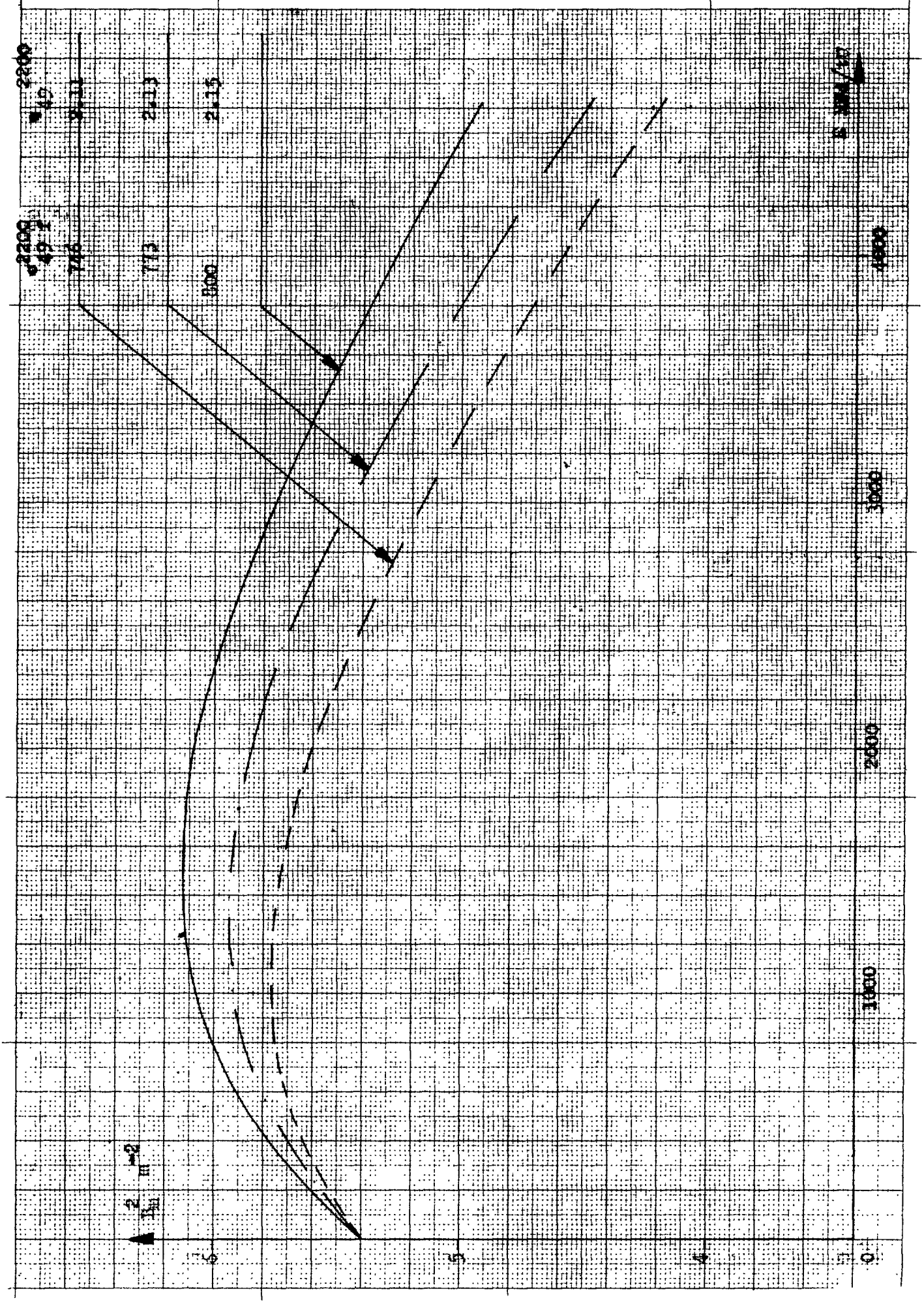

List of reports published in the AE-series.

1. Calculation of the geometric buckling for reactors of various shapes. By N. G. Sjöstrand. 1958. 23 p. Sw cr. 3:-

2. The variation of the reactivity with the number, diameter and length of the control rods in a heavy water natural uranium reactor. By H. Mc Cririck. 1958. 24 p. Sw. cr. 3:-

3. Comparison of filter papers and an electrostatic precipitator for measurements on radioactive aerosols. By R. Wiener. 1958. 4 p. Sw. cr. 4:-

4. A slowing-down problem. By I. Carlvik and B. Pershagen. 1958. 14 p. Sw. cr. 3:-

5. Absolute measurements with a 4 π-counter. (2nd rev. ed.). By Kerstin Martinsson. 1958. 20 p. Sw. cr. 4:-

6. Monte Carlo calculations of neutron thermalization in a heterogeneous system. By T. Högberg. 1959. 13 p. Sw. cr. 4:-

8. Metallurgical viewpoints on the brittleness of beryllium. By G. Lagerberg. 1960. 14 p. Sw. cr. 4:-

9. Swedish research on aluminium reactor technology. By B. Forsén. 1960. 13 p. Sw. cr. 4:-

10. Equipment for thermal neutron flux measurements in Reactor R2. By E. Johansson, T. Nilsson and S. Claesson. 1960. 9 p. Sw. cr. 6:-

11. Cross sections and neutron yields for U^{233}, U^{235} and Pu^{239} at 2200 m/sec. By N.G. Sjöstrand and J.S. Story. 1960. 34 p. Sw. cr. 4:-

12. Geometric buckling measurements using the pulsed neutron source method. By N.G. Sjöstrand, J. Mednis and T. Nilsson. 1959. 12 p. Sw. cr. 4:-

13. Absorption and flux density measurements in an iron plug in R1. By R. Nilsson and J. Braun. 1958. 24 p. Sw. cr. 4:-

14. GARLIC, a shielding program for GAmma Radiation from LIne- and Cylinder-sources. By M. Roos. 1959. 36 p. Sw. cr. 4:-

15. On the spherical harmonic expansion of the neutron angular distribution function. By S. Depken. 1959. 53 p. Sw. cr. 4:-

16. The Dancoff correction in various geometries. By I. Carlvik and B. Pershagen. 1959. 23 p. Sw. cr. 4:-

17. Radioactive nuclides formed by irradiation of the natural elements with thermal neutrons. By K. Ekberg. 1959. 29 p. Sw. cr. 4:-

18. The resonance integral of gold. By K. Jirlow and E. Johansson. 1959. 19 p. Sw. cr. 4:-

19. Sources of gamma radiation in a reactor core. By M. Roos. 1959. 21 p. Sw. cr. 4:-

20. Optimisation of gas-cooled reactors with the aid of mathematical computers. By P. H. Margen. 1959. 33 p. Sw. cr. 4:-

21. The fast fission effect in a cylindrical fuel element. By I. Carlvik and B. Pershagen. 1959. 25 p. Sw. cr. 4:-

22. The temperature coefficient of the resonance integral for uranium metal and oxide. By P. Blomberg, E. Hellstrand and S. Hörner. 1960. 25 p. Sw. cr. 4:-

23. Definition of the diffusion constant in one-group theory. By N.G. Sjöstrand. 1960. 8 p. Sw. cr. 4:-

25. A study of some temperature effects on the phonons in aluminium by use of cold neutrons. By K-E. Larsson, U. Dahlborg and S. Holmryd. 1960. 32 p. Sw. cr. 4:-

26. The effect of a diagonal control rod in a cylindrical reactor. By T. Nilsson and N.G. Sjöstrand. 1960. 4 p. Sw. cr. 4:-

28. RESEARCH ADMINISTRATION: A Selected and annotated bibliography of recent literatur. By E. Rhenman and S. Svensson. 1960. 49 p. Sw. cr. 6:-

29. Some general requirements for irradiation experiments. By H.P. Myers and R. Skjöldebrand. 1960. 9 p. Sw. cr. 6:-

30. Metallographic Study of the Isothermal Transformation of Beta Phase in Zircaloy-2. By G. Östberg. 1960. 47 p. Sw. cr. 6:-

32. Structure investigations of some beryllium materials. By I. Fäldt and G. Lagerberg. 1960. 15 p. Sw. cr. 6:-

33. An Emergency Dosimeter for Neutrons. By J. Braun and R. Nilsson. 1960. 32 p. Sw. cr. 6:-

35. The Multigroup Neutron Diffusion Equations /1 Space Dimension. By S. Linde. 1960. 41 p. Sw. cr. 6:-

36. Geochemical Prospecting of a uraniferous bog deposit at Masugnsbyn, Northern Sweden. By G. Armands. 1961. Sw.cr. 6:-

37. Spectrophotometric Determination of Thorium in Low Grade Minerals and Ores. By A-L. Arnfelt and I. Edmundson. 1960. 14 p. Sw. Cr. 6:-

38. Kinetics of Pressurized Water Reactors with Hot or Cold Moderators. By O. Norinder. 1960. Sw.Cr. 6:-

39. The dependence of the resonance on the Doppler effect. By J. Rosén. 1960. Sw. Cr. 6:-

40. Measurements of the fast fission factor (ε) in UO_2-elements By O. Nylund. 1960. Sw. cr. 6:-

44. Hand monitor for simultaneous measurement of alpha and beta contamination. By I.Ö. Andersson, J. Braun and B. Söderlund. 1960. Sw.cr. 6:-

46. The magnetism of MnB and its variation with the temperature. By N. Ländquist and H.P. Myers. 1960. Sw.cr. 6:-

47. An experimental study of the scattering of slow neutrons from H_2O and D_2O. By K.E. Larsson, S. Holmryd and K. Otnes. 1960. Sw.cr. 6:-

48. The resonance integral of thorium metal rods. By E. Hellstrand and J. Weitman. 1960. Sw.cr. 6:-

49. Pressure tube and pressure vessels reactors; certain comparisons. 1961. By P.H. Margen, P.E. Ahlström and B. Pershagen. Sw.cr. 6:-

50. Phase transformations in a uranium-zirconium alloy containing 2 weight per cent zirconium. By G. Lagerberg. 1961. Sw.cr. 6:-

Additional copies available at the library of AB Atomenergi, Studsvik, Tystberga, Sweden. Transparant microcards of the reports are obtainable through the International Documentation Center, Tumba, Sweden.

Affärstryck, Stockholm 1961